Aerosol Retrieval over Land from AVHRR Data—Application for Atmospheric Correction

Brent Holben, Eric Vermote, Yoram J. Kaufman, Didier Tanré, and Virginia Kalb

Abstract—**Correction of AVHRR imagery for the aerosol effect requires retrieval of the aerosol loading from the images. In this paper two retrieval algorithms that were previously developed for Landsat are modified for the AVHRR. The methods which determine the aerosol optical thickness over land surfaces from AVHRR band 1 data independent of ancillary information are described. The first method retrieves aerosols based on the atmospheric effect on the path radiance This method requires the surface reflectance to be 0.02±0.01, which is found over forests in the red channel. Two techniques are used to screen an AVHRR scene for pixels that have this low reflectance. One is based on selecting the lowest NDVI or by selecting the minimum 3.75-μm radiance. The qualifying requirements for these techniques are discussed and the method demonstrated to retrieve aerosol optical thicknesses to $\sim \pm 0.1$. The second method uses the change in contrast for several scenes to determine the change in the optical thickness between the scenes. A reference scene allows absolute determination. The method has an rms error of ~ 0.1. The two methods are discussed with respect to other methods as well as their implications for global scale aerosol monitoring and atmospheric correction.**

I. Introduction

The Advanced Very High Resolution Radiometers (AVHRR) on board the NOAA series of satellites have been in continuous polar orbit since 1979. Spectral data of the Earth's surface is acquired at 1- and 4-km resolutions in five spectral bands ranging from the visible and near-infrared, middle-IR and thermal bands four times daily for the thermal bands and depending on latitude up to twice daily from solar bands from two orbiting platforms. This has created a remarkable global data set beginning in 1979 and will extend into the next century in which the potential for monitoring global scale ocean, terrestrial, and atmospheric processes is being developed. An important aspect of that development is assessing aerosol concentrations, distributions, and optical characteristics. This paper reports on several techniques to assess aerosol optical thickness over land from AVHRR visible and near-IR data.

Decoupling the atmospheric effects (water vapor and ozone absorption, and aerosol and molecular scattering) from the terrestrial surface signal has been fairly successfully achieved by many authors ([1] for a review). All but aerosols can be taken into account accurately from ancillary data sources and used in the correction. This has led to the development of a family of methods for aerosol retrievals in which the radiance from a dark target of known reflectance (ocean) is inverted in an appropriate aerosol model to obtain the correct aerosol optical thickness for that surface reflectance. This approach, begun over oceans using Landsat MSS [2], developed into a routine NOAA product using weekly AVHRR data sets [3].

Virtually all procedures for retrieving aerosols from satellite data over land areas require *a priori* knowledge of the surface and/or require a change detection procedure. Typically these have been developed using high resolution Landsat or SPOT data. For example, the ocean method applied over dense, dark green vegetation showed good results for forests near Chesapeake Bay using Landsat MSS [4]. A complimentary technique was developed using TM data which selects invariant targets and relates the change in contrast between the invariant targets to the aerosol optical thickness on a reference day [5]. In a more simplified approach, termed the brightness method, the apparent change in reflectance above a pixel from one day to another is related to the difference in optical thickness between the two days assuming the surface reflectance did not change. The method could apply when neither dense vegetation is present in the image, and the surface reflectance is too uniform to apply the contrast method; however, it requires precise registration and there is no methodology to separate an atmospheric effect from a surface effect. This method was developed and applied to GOES [6] and the AVHRR [7], [8] and, therefore, will not be discussed in this paper. This method though powerful for higher resolution imagery may not work for the AVHRR due to the large footprint

A different strategy (radiometric rectification) foregoes the derivation of the aerosol optical thickness but normalizes the radiances from several Landsat TM images of the same target area taken from several years under a variety of atmospheric conditions and calibrations [9]. The scenes were dynamically stretched to the same contrast range thereby assuming the extreme features did not change temporally but could change spatially within the scene.

Aerosol retrievals over land and subsequent atmospheric corrections to AVHRR data which are derived from the satellite imagery, to the best of our knowledge have not been published. Correction for reduced resolution Landsat data were proposed [4] and derivation of the change in the aerosol optical thickness between several TM images were demonstrated by Tanré [5]. In this paper, we shall discuss the conceptualization (Section II) and implementation (Section III) of these techniques to the AVHRR incorporating the 3.75-μm channel not available on the Landsat platform. Several applications and comparisons with ground measurements are given through a sensitivity study of the expected accuracies for the AVHRR and broad

Manuscript received September 26, 1991; revised November 1, 1991.

The authors are with the NASA/Goddard Space Flight Center, Greenbelt, MD 20771.

IEEE Log Number 9105382.

validation is left for future investigations. Finally the methods are compared, enhancements suggested and implications for AVHRR atmospheric corrections are discussed in Section IV.

II. Conceptualization of Aerosol Retrievals

The methods for aerosol retrievals are based on determination of the concentration of atmospheric aerosol (or the aerosol optical thickness, τ_a) from radiances taken from the image itself. The atmospheric effect on the image, described by:

$$L(\tau_a, \mu_s, \mu_v, \phi) = L_o(\tau_a, \mu_s, \mu_v, \phi) + F_d(\tau_a, \mu_s)T(\tau_a, \mu_v)\rho/[1 - s(\tau_a)\rho] \quad (1)$$

is composed of two parts: (1) The atmospheric path radiance L_o due to photons scattered by the atmosphere to the sensor without being reflected by the surface, and (2) The atmospheric effect on the transmission of the downward flux, F_d, and the upward transmission, T. μ_s,$\mu_v$and ϕ describe the zenith illumination, and viewing and azimuthal conditions respectively. $[1 - s(\tau_a)\rho]$ describes the multiple interaction between the ground and atmosphere where $s(\tau_a)$ is the spherical albedo and ρ is the surface reflectance. Both atmospheric effects were used in the past to determine the aerosol optical thickness. In the following we shall review these techniques.

A. Determination of the Aerosol Optical Thickness Using the Path Radiance

In order to determine the aerosol optical thickness from the path radiance, the second term in (1) has to be small, so that the uncertainty in the surface reflectance, ρ, will have a minimal effect on the determination of τ_a. The method was applied over dark surfaces, e.g., oceans and inland water bodies using Landsat data [2], [10], [11] and over dark vegetation [4]. The much lower resolution of the AVHRR data limits the presence of pure inland water pixels, and, therefore, this method is not appropriate for AVHRR data.

A variety of forests, forming dense, dark green canopies have low reflectance, 1–2%, in the red channel, e.g., deciduous forest [4], coniferous forest [12], [13], hardwood and pine forests [14], [15], and tropical forests [16]. Therefore, forests or large patches of forests in generally urban or agricultural areas, can be used to derive the aerosol optical thickness and apply atmospheric corrections. This method we term dense dark vegetation (DDV) and appears appropriate for the coarse resolution AVHRR data.

The accuracy of the determination of the aerosol optical thickness using the path radiance depends on the accuracy of the assumed reflectance of the dark objects (e.g., vegetation or water) and on the ability to estimate the aerosol scattering phase function and single scattering albedo. Recent compilation of aerosol optical thickness measurements with simultaneously measured path radiance [17] shows that the empirical error in the derivation of optical thickness from the path radiance, due to uncertainty in the phase function is around $\Delta\tau_a = \pm 0.05$. The uncertainty in the phase function is a result of variation in the aerosol size distribution as well as particle shape and composition. The total error in this method (including the effect of uncertainty in the surface reflectance) for dense dark vegetation (assuming a good calibration) was estimated as $\Delta\tau_a = \pm 0.10$ [4] for Landsat MSS. In the process of correcting the image for the atmospheric effects, the errors due to uncertainty in the aerosol phase function cancel partially [4] since the same phase function that is used to derive the aerosol optical thickness is subsequently used in the correction process. As a result, the error in the derived surface reflectance is mainly driven by the accuracy of the assumed reflectance of the dark surface ($\Delta\rho = \pm 0.01$). Extrapolation of the optical thickness to other channels (from the red to the near IR) can be done with an uncertainty of $\Delta\tau_a = \pm 0.05$ and for the path radiance with uncertainty of $\Delta L = \pm 0.002 \cdot F_0/\pi$ [17].

The method can be applied to images for which it is *a priori* known that dense vegetation is present, accounting for the geographic location and season in which the image was taken (for an estimate of geographic distribution see Fig. 12 of [4]). Some minimal fraction of pixels covered by the dense vegetation has to be assumed (the actual fraction may be larger). It is further assumed that the spatial distribution of these pixels is sufficient to cover any spatial variability in the aerosol concentration. Two approaches are studied to determine, on a statistical basis, which pixels are covered by dense dark vegetation.

1) Determination Based on the Vegetation Index: This method developed using MSS data is described in detail by Kaufman and Sendra [4]. Following is a brief summary of the method modified for the AVHRR band 1. The normalized difference vegetation index (NDVI) can be used to determine pixels that have the densest, greenest, darkest vegetation in the image. The NDVI is based on the ratio of the difference between the satellite level near-IR and the red band radiances divided by their sum. Fundamentally it is related to changes in chlorophyll content and leaf structure in green vegetation [18]. The absolute value of the NDVI depends on the atmospheric effect [19], [1], viewing and illumination geometry [20], and surface bidirectional reflectance [14], [13], [21], [1]. As long as the image to be analyzed is small, aerosol concentration is more likely to be uniform, geometrical effects will be minimized, and pixels that correspond to the densest vegetation will have the highest NDVI values. Uniformly distributed water vapor across a scene is also required and is more likely for smaller sized images. Pixels that correspond to dense, dark vegetation (DDV) are identified from the vegetated pixels, as pixels having the lowest reflectance in the near IR. These pixels are expected to have low well-defined reflectance in the visible band that can be used to determine the aerosol optical thickness. For images with variable aerosol and water vapor concentrations, the DDV method will tend to select pixels with low aerosol and low water vapor concentrations [4] given similar surface reflectance. The method is expected to be useful for areas of uniformly distributed atmospheric effects

2) Determination Based on Radiance at 3.75 μm: Radiance at 3.75 μm is affected both by thermal emission and by reflection of the weak sunlight in this wavelength. Depending on the value of the surface reflectance and temperature, either of these two effects can dominate. The complex characteristics of this channel make it hard to use, but some widely different

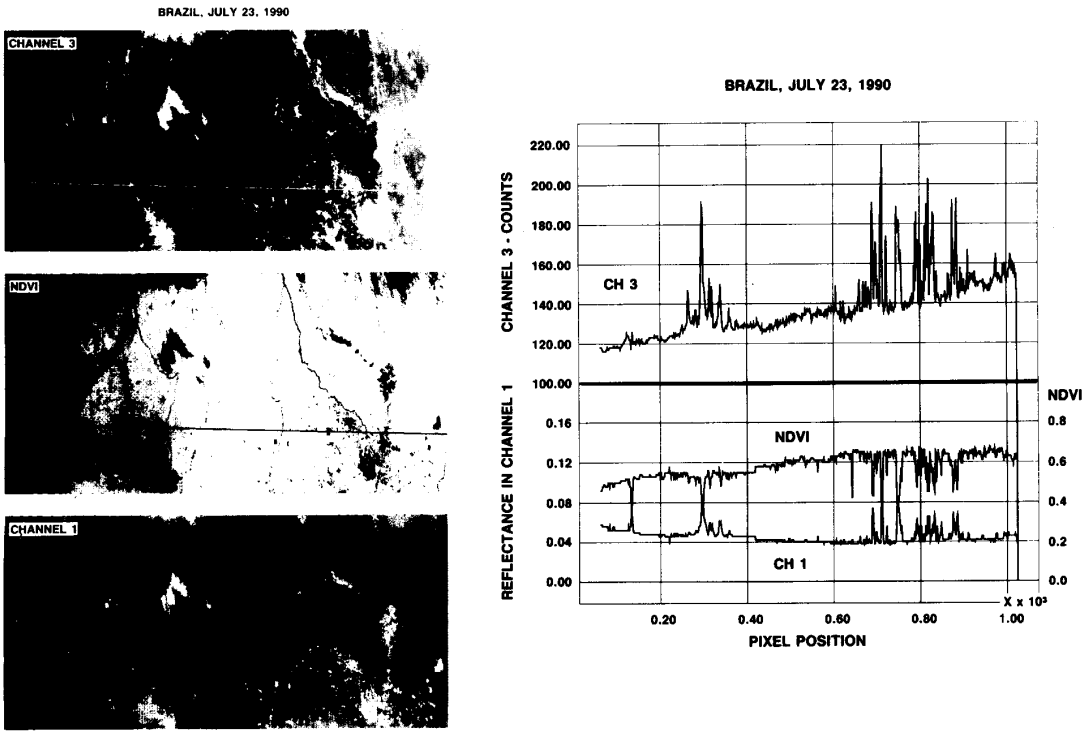

Fig. 1. AVHRR bands 1 and 3 and NDVI are plotted vs. scan angle for a transect across the southern Amazon forest which is dominated by dense dark vegetation. Note the increased sensitivity in band 3 relative to the NDVI for surface variations.

applications do emerge. This channel on the AVHRR is used to determine the size/phase of cloud drops [22], is very sensitive to variation in the surface temperature [23], and is the most sensitive channel to detect the difference between mature forest and green deforested area [24], [25].

This last approach suggests application to aerosol retrieval using the DDV. In an image of mixed surface cover, excluding water bodies, clouds, and snow, forest is expected to have the lowest radiance in this channel. Due to evaporation, forest is usually cooler than regions with lower density vegetation or bare soil, vegetation has low reflection in this channel due to the absorption of liquid water in live vegetation, and forest decreases this reflection even further by trapping incoming sunlight due to the multilayer canopy structure. These characteristics are demonstrated for the visible and 3.75-μm channels and NDVI in a remarkably cloud free AVHRR scene over the Amazon forest (Fig. 1) It is shown that variation in the reflectivity of the red channel, caused by variation in the surface cover, are correlated with the vegetation index, and are even more enhanced in the value of the 3.75-μm channel, which has a smaller scan angle effect.

Since most aerosol types have small particle size, and small imaginary index in this wavelength range [26]–[28], [16] the aerosol layer is mostly transparent in this wavelength. Therefore, the selection of dense vegetation pixels is expected to be nearly independent of the aerosol loading and the 3.75-μm channel should be better than the NDVI in selecting the dense dark vegetation pixels where aerosol concentrations vary. Note that desert dust may behave differently in this respect due to the large particle size.

B. Determination Based on Atmospheric Transmission (Contrast Reduction)

Determination of the aerosol optical thickness from the atmospheric transmission (second term in (1)) is based on the ratio of the transmission among several images and is termed contrast reduction. Tanré [5] suggested and applied the method to TM images taken over an arid region. The variation in the transmission is determined from the variation of the difference between the radiance from pixels located a specified distance apart. From (1) the difference of apparent radiance ΔL^*_{ij} between two adjacent pixels (i,j) and $(i,j+1)$, where i and j are the geographical coordinates expressed in line and column numbers, is related to the actual ground reflectance difference $\Delta\rho_{ij}$ by

$$\Delta L^*_{ij}(\tau_a,\mu_s,\mu_v) \simeq \Delta\rho_{ij}\frac{T(\tau_a,\mu_v)\,F_d(\tau_a,\mu_s)}{1.- <\rho> s(\tau_a)\cdot 2} \qquad (2)$$

where $\langle\rho\rangle$ is the mean reflectance of the two pixels.

If the method is applied to a group of images that includes a relatively clear image (for which the optical thickness can be estimated or was measured), the actual $\Delta\rho_{ij}$ can be derived and the optical thickness for each of the images can be estimated from (2), [5]. The derived optical thickness is independent of the aerosol scattering phase function, but

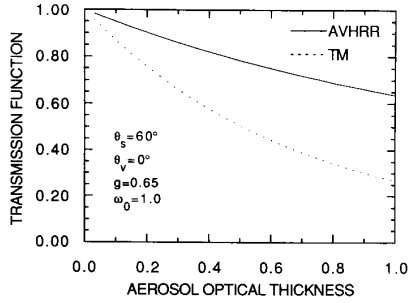

Fig. 2. The transmission function response for AVHRR band 1 and TM 3 are simulated for a large range of aerosol optical thickness. The sensitivity of the AVHRR band, although not as great as the TM, is adequate for retrieval using the transmission function method.

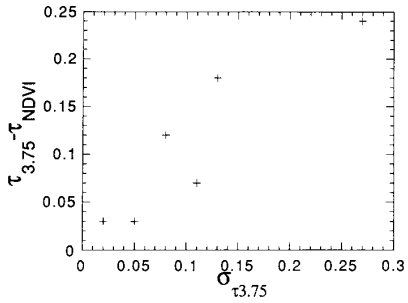

Fig. 3. The τ_a difference between the 3.75 and NDVI methods is plotted against the standard deviation ($\sigma_{\tau 3.75}$) of the aerosol optical thickness for scenes analyzed. As the aerosol inhomogeneity increases (high $\sigma_{\tau 3.75}$) the difference between the two methods increases illustrating the utility of the 3.75-μm method under these conditions.

depends on the single scattering albedo, ω_0, and asymmetry parameter of the aerosol.

The reduction in contrast for TM and AVHRR resolution as a function of the aerosol optical thickness, for $\theta_s = 60°$, a nadir observation and a continental aerosol model was simulated (Fig. 2). The contrast reduction is 40% lower for the AVHRR but still large enough for hazy or dusty conditions in order to be applied in arid or semiarid regions where large and variable aerosol concentrations prevail [29].

To express the contrasted character of the target, ($\Delta\rho_{ij}$), we use the structure function concept, noted $Fs(d)$, and defined by

$$Fs(d)^2 = \frac{1}{n*(m-d)} \sum_{i=1}^{n} \sum_{j=1}^{m-d} (\rho_{ij} - \rho_{i,j+d})^2 \quad (3)$$

where d is the distance between the pixels and $n^*(m-d)$ is the total number of pixels within the target for the structure function $F^*s(d)$. From (2) and (3), the structure function observed from the satellite $F*s(d)$ and the actual structure of the surface $Fs(d)$ are related by

$$F*s(d) \simeq Fs(d)\frac{T(\tau_a,\mu_v)F_d(\tau_a,\mu_s)}{1-A*s(\tau_a)} \quad (4)$$

where A is the mean albedo of the target [30].

Provided that $Fs(d)$ is known and invariant, the satellite measurements allow us to estimate the aerosol optical thicknesses by means of the transmissions functions of (4).

III. Demonstration of Aerosol Optical Thickness Retrievals

The two methods (DDV and Contrast Reduction) generally apply to different cover types. The DDV obviously is appropriate in areas where dense dark vegetation is at least distributed in patches of greater than 1 pixel size across a scene. The contrast reduction method applies easily to areas devoid of vegetation as long as large contrasts in the surface reflectance exist and remain invariant between scenes. For this reason we have chosen two sites, the Amazon basin for the DDV study and the Sahel in Mali for the contrast reduction study. Some ground truth data is available at both sites.

A. The Dense Dark Vegetation Method

This method was applied to four, 1989 AVHRR 2 × 2 degree scenes with a 1-km pixel resolution over the Amazon basin in Brazil. The aerosol optical thickness was measured by the authors on days 247 and 249. The two sites, Alta Floresta and Santarem, were chosen in the Amazon basin because they contain large tracts of dense forest canopies. In the area of our ground observations, significant deforestation by burning resulted in large areas of nonforest canopies and bare ground. A third site of intensive forest burning was chosen over the state of Rondonia to illustrate differences in the methods under conditions of spatially variable concentrations of aerosols. Both DDV methods were applied as described previously. Ground observations were made from a five-band sun photometer taken at a single location within the respective scenes we analyzed. Therefore, some discrepancy is expected between the ground observations and the AVHRR retrieved aerosol optical thicknesses.

The retrieved aerosol optical thickness in band 1 was computed for the NDVI and 3.75 μm techniques according to the criteria in the previous section. Cloud screening was applied on all dates using a simple interactive thermal threshold at 11.0 μm and a primitive cloud shadow approximation based on an assumed cloud height and illumination direction. This eliminated from 20 to 80% of all pixels for the various scenes due to the afternoon broken cumulus cloud layer.

The optical thicknesses measured for each site and the mean values retrieved by each method (days 247 and 249) generally agree to within 0.2. For the uniformly distributed optical thickness (standard deviation in the 3.75-μm method is < 0.05), the NDVI and 3.75-μm methods agree within $\Delta\tau_a = 0.03$. For a very nonuniform day (252, 1987) with observed smoke plumes, $\sigma_{3.75} = 0.27, \tau_{a3.75}$ is larger than τ_{aNDVI} by 0.24 (Table I). For day 247 the mean value of the NDVI method is within 0.01 of the ground observation and the 3.75-μm method exceeds the ground observation by 0.11; however, the standard deviation for the 3.75-μm method is large (Table I). This is illustrated by plotting the difference of the mean retrieved aerosol optical thickness by the two methods vs. the standard deviation from the 3.75-μm method (Fig. 3). A clear trend of increasing inhomogeneity (larger

TABLE I
COMPARISON BETWEEN AEROSOL OPTICAL THICKNESS DERIVED IN EACH OF THE METHODS AND GROUND MEASUREMENTS.

Day/yr.	Geometry(°) $\theta_s/\theta_v/\phi$	Aerosol Optical Thicknesses (τ_a) NDVI Method	3.75-μm Method	ground obs.	cloud fraction	Location/comments
247/89	40.9/-43.4/139	0.39±0.02	0.51±0.08	0.40	0.70	Alta Floresta
249/89	35.9/-17.1/137	0.40±0.02	0.58±0.13	0.52	0.26	Alta Floresta
249/89	35.0/-34.2/148	0.36±0.04	0.33±0.02	0.16	0.67	Santarem
250/89	33.6/-1.0/111	0.51±0.02	0.58±0.11	ND	0.68	Alta Floresta
259/89	34.2/-9.4/143	0.33±0.02	0.36±0.05	ND	0.79	Alta Floresta
252/87	49.6/-9.4/72	0.32±0.09	0.56±0.27	ND	0.18	smoke plumes

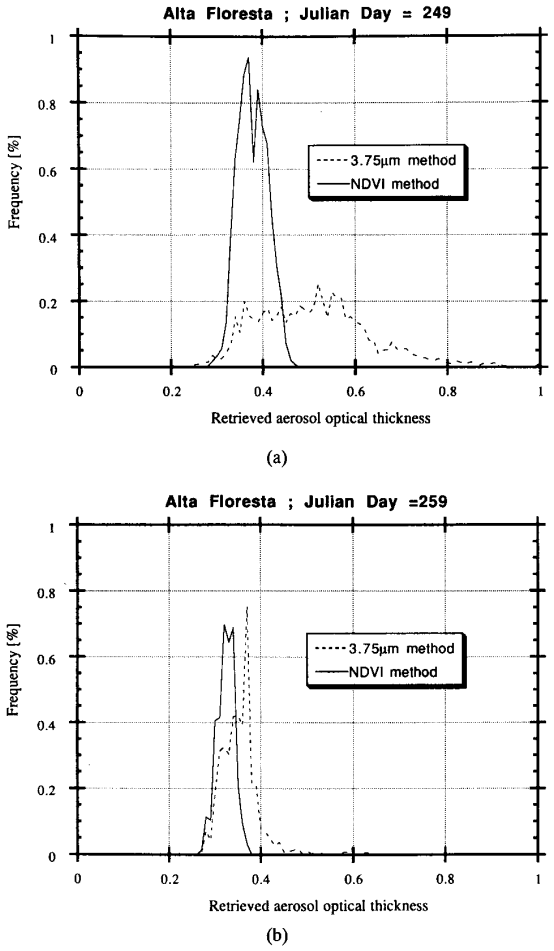

Fig. 4. Frequency histograms of NDVI and channel 3 methods for aerosol retrieval on a hazy day (a) and clear day (b) in Alta Floresta, Brazil.

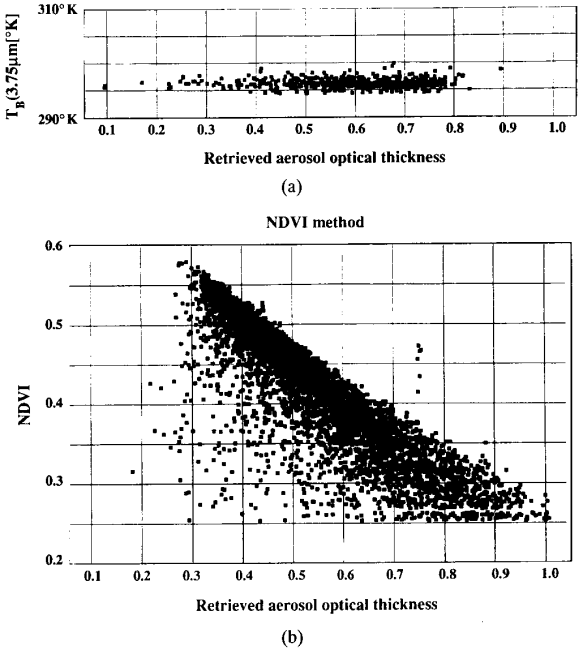

Fig. 5. The sensitivity of the 3.75-μm (a) and NDVI (b) methods to aerosol heterogeneous distributions is illustrated. For optical thicknesses from 0.25 to 1.0 the NDVI varies by a factor of two and 3.75 μm method by only 4°K.

$\sigma_{3.75}$ results in a larger disparity between the methods. A frequency histogram of day 249 at Alta Floresta indicates the 3.75-μm method retrieves a much broader range of aerosol optical thicknesses than does the NDVI on this date suggesting a lack of uniformity in the aerosol optical thickness across the scene which is a violation of the basic assumption of the NDVI method (Fig. 4(a)). In contrast, the frequency histograms for day 259 are nearly identical and the range in retrieved aerosol optical thickness is small (Fig. 4(b)). In this case, the techniques appear equivalent.

The sensitivity of the two methods to aerosol nonuniformity is further illustrated by plotting the brightness temperature at 3.75 μm and the NDVI for the selected DDV pixels in each method vs the retrieved aerosol optical thickness for day 249 (Fig. 5). By relaxing the thresholds for the NDVI technique, the range of the retrieved optical thicknesses was matched to the range in retrieved values using the 3.75-μm technique. While the NDVI decreases as a function of τ_a, the $T_{3.75}$ brightness temperature is independent of τ_a illustrating the advantage of the 3.75-μm technique for nonuniform aerosol layers (Fig. 5). Under these circumstances of nonuniform aerosol distribution over a relatively constant terrain elevation and airmass, the 3.75-mm method would be more reliable. The results clearly demonstrate the requirement for a uniformly distributed aerosol optical thickness over the scene in question

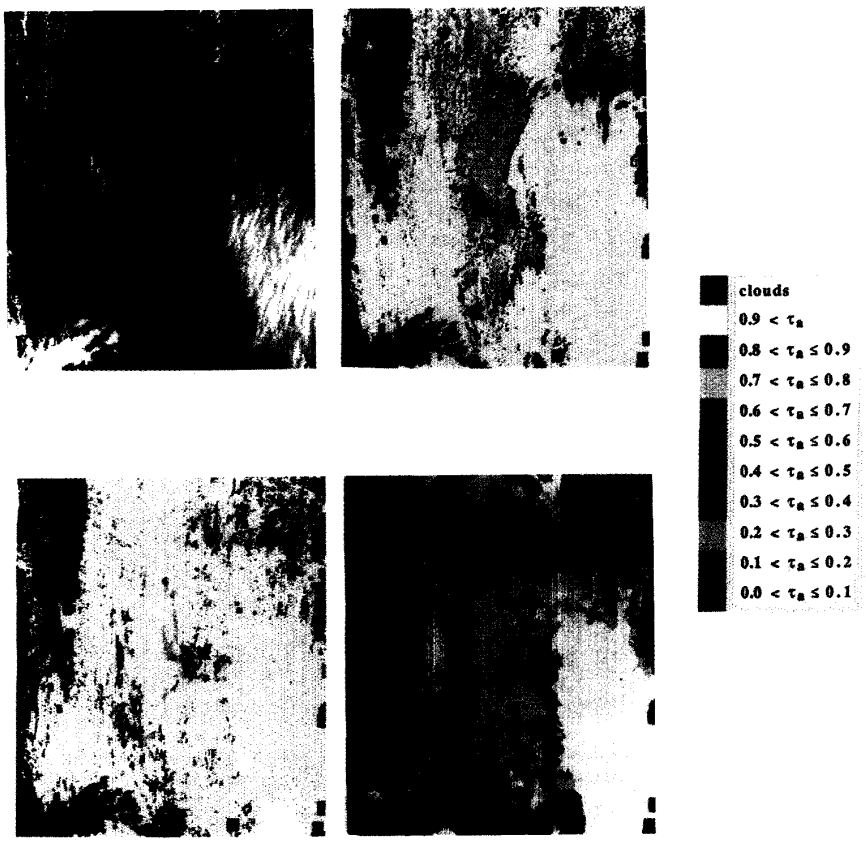

Fig. 6. Intense burning over Rondonia, Brazil created a nonuniform distribution of aerosols. The AVHRR visible channel (a) illustrates the location of smoke plumes relative to the clear areas; A cloud mask is applied to the remaining color panels (purple). The NDVI retrieval method (b) retrieved lower optical thicknesses than the 3.75-μm method (c). The 3.75-μm retrieval is interpolated across the scene (d) to illustrate the scene used for an atmospheric correction.

to successfully retrieve the aerosol optical thickness by the NDVI method.

The AVHRR imagery from Day 252 of 1987 showed well-defined smoke plumes over the Brazilian state of Rondonia [31] and, therefore, the optical thickness changed dramatically across the 2 × 2 degree scene considered. Both methods were used to retrieve the aerosol optical thickness. A cloud mask indicates a few clouds near the margins of the image (Fig. 6(a)). The retrieved optical thicknesses for the NDVI method are in the clear air away from the plumes (Fig. 6(b)) resulting in a low mean optical thickness for the image of 0.32 (Table I), in contrast to the higher optical thicknesses retrieved in the vicinity of the plumes with the channel 3 method (Fig. 6(c)) with a mean retrieved value of 0.56 for the scene. After interpolation, the 3.75-μm method produces a relatively complete distribution of aerosol optical thickness across this scene in which the retrieved aerosol optical thickness varies from 0.3 to 1.0 (Fig. 6(d)) and the smoke plumes' are clearly seen.

The last site considered is in Santarem, Brazil. Ground observations made at the Airport approximately 1.5 h after the AVHRR overpass showed an aerosol optical thickness of 0.16 for AVHRR band 1 and the visibility was observed to be greater than 15 km for the region with numerous small cumulus. The retrieved values for both methods are similar, near 0.3 (Table I, double the measured value). There can be several factors contributing to the disparity between the retrieved and measured values. First, the measured value is simply one observation that may not be representative of the retrieval area. The AVHRR is viewing in the hot spot direction for the Santarem scene. The magnitude of the effect is not known although the direction will be to overestimate the retrieved aerosols. Because the area surrounding Santarem is populated, we may well expect cultural activities to increase the surface reflectance above the assumed 0.02, thereby increasing the retrieved value of the aerosol optical thickness.The Santarem overpass, as with many AVHRR afternoon overpasses, is contaminated with cumulus formations which increase the likelihood of incorporating subpixel clouds in the "cloud free" radiances used for the retrievals. This could also lead to overestimation of the retrieved aerosol optical thickness. It is encouraging to be able to retrieve reasonable though probably high τ_a values between the clouds. Recognizing the effect of subpixel clouds, we are investigating methods to minimize this effect.

Because our lack of knowledge of the true surface reflectance in band 1 for various conditions and our current

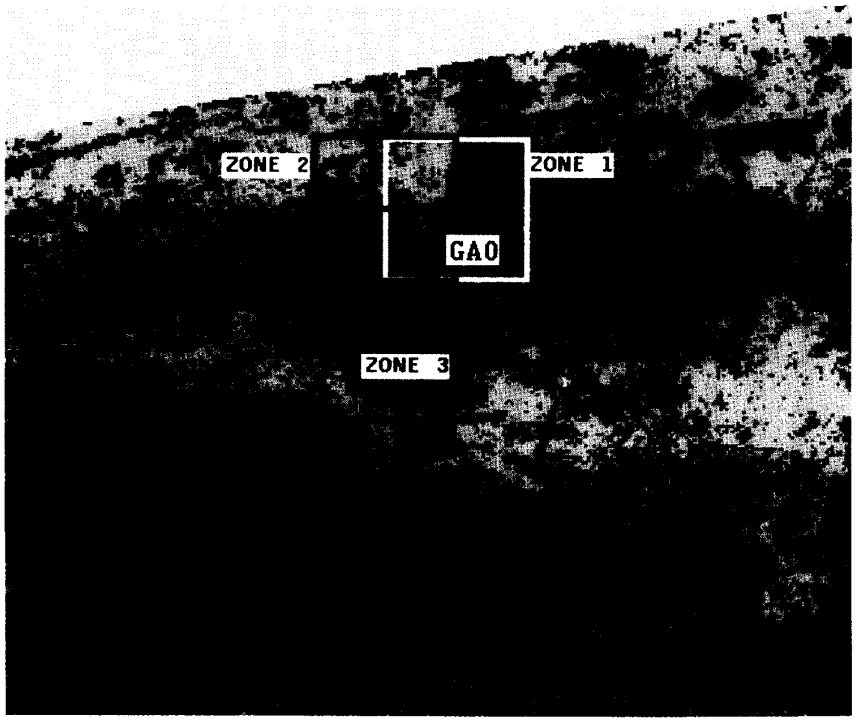

Fig. 7. The NDVI computed from the reference image shows the location of the three zones each 40 LAC pixels square used for the contrast reduction method. The ground observation site at Gao, Mali is common to all zones.

uncertainty in setting thresholds *a priori* for both methods, we used the 5S code [32] to estimate the uncertainty in retrieved aerosol optical thickness for a 0.01 departure from the assumed 0.02 surface reflectance. The difference is approximately 0.15 and considering other sources of error a deviation of 0.2 from the true value in some cases is not unreasonable.

B. The Contrast Reduction Method

The method is applied to images where it is possible to find invariant targets, typically arid and semiarid regions as, in our case, the Sahel of Mali, where the DDV method cannot be applied. We selected six AVHRR images in which simultaneous ground measurements are available [29], one at the end of the growing season (86/10/3, day 276) and five within the dry season 86/12/09 (day 343), 86/12/10 (day 344), 86/12/19 (day 353), 87/01/05 (day 005) and 87/01/15 (day 015). The selections have similar geometrical conditions and widely varying atmospheric conditions (Table II).

Within the image, three subzones were selected (Fig.7). Zone 1 (white box) has two prominent features, the Niger river and a low range of the mountains in the east; zone 2 (the red box), west of the first includes the Niger river and bright pixels to the north; zone 3 (green box) was south includes a small portion of the Niger river but has no other prominent features (Fig. 7). Gao airport, the site of the ground observations is common to all zones and is indicated by (+). The three zones are 50 by 50 pixels in size or about 80 km square; the pixel size is 1.5 km after mapping. The data were mapped and registered with one pixel accuracy to have the same geographical area for the different days.

TABLE II
GEOMETRICAL AND ATMOSPHERIC CONDITIONS AT GAO, MALI FOR THE 6 DAYS.

Day of Yr.	θ_s	θ_v	ϕ	τ_a	UH_2O
276	54.4	45.6	50	0.40	4.20
343	60.0	14.0	34	0.11	1.53
344	58.0	7.2	210	0.08	1.44
353	58.4	1.6	210	0.63	0.66
005	60.0	30.4	33	0.40	1.18
015	56.8	17.2	32	0.35	1.27

Results of the structure function (3) are plotted versus distance from any given pixel within the three zones. This illustrates how the structure function changes due to the influence of variable aerosol loading on each day and the importance of selecting an area of sufficient contrast to observe the atmospheric effect. For zone 1 (Fig. 8(a)), the magnitude of the structure functions is in agreement with ground optical thickness measurements (Table II). The largest structure is observed for the clearest day (344) and no difference for day 343 which has similar atmospheric conditions. Days 276, 005, and 015 are all lower and have magnitudes commensurate with the measured intermediate aerosol optical thicknesses and lastly the most turbid day (353) has the lowest structure function. The same conclusions apply to zone 2 except day 276 appears as the most turbid day (Fig. 8(b)). The magnitude

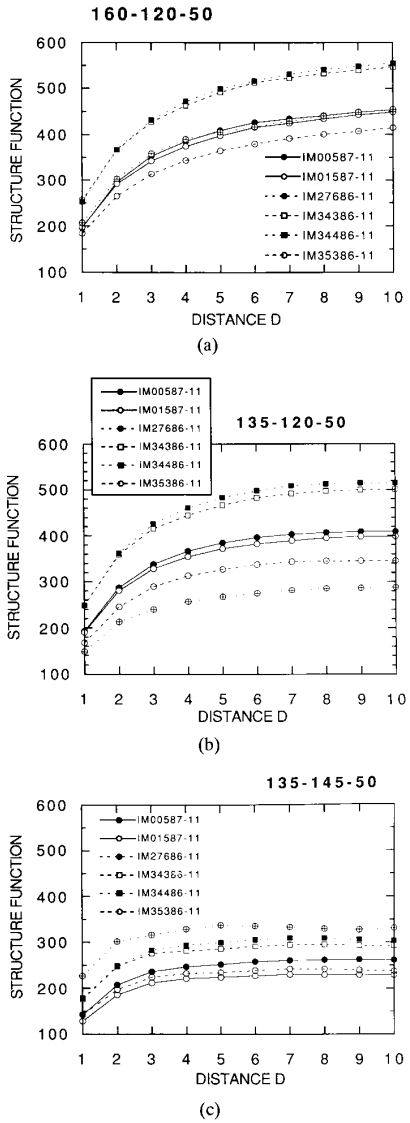

Fig. 8. The structure function is plotted against the distance D for zones 1 through 3 (a, b, and c). Note the decrease in structure function for zone 3 compared to zones 1 and 2.

of the structure is slightly smaller (10%) for all days than for zone 1 because the mountain feature is absent. For zone 3 (Fig. 8(c)), the magnitude is only half that of zone 1, and the different days are not ordered in relation to the ground aerosol optical thickness.

Using the clearest day (344) as the reference day (Table II) and assuming the surface as invariant, from (4), plots of $F^*s(d)$ as a function of $F^*s(d)$ for day 344 should be straight lines. Slopes should be directly related to the function $T(\tau, \mu_v)Fd(\tau, \mu_s)$. Zone 1 and 2 (Figs. 9(a) and (b)) show excellent linearity as indicated by theory, except day 276. Linear correlation coefficients for each date are greater than 0.99920 for all days but 276 for zones 1 and 2 and generally are

TABLE III
LINEAR CORRELATION COEFFICIENTS (R) OF THE STRUCTURE FUNCTION FOR EACH DATE VS THE REFERENCE DATE, 344. NOTE THE LOW VALUES FOR ZONE 3 AND DAY 276 FOR ALL ZONES.

Day of Yr.	Zone 1 (r)	Zone 2 (r)	Zone 3 (r)
276	0.99910	0.99866	0.98011
343	0.99983	0.99967	0.99749
344	1.00000	1.00000	1.00000
353	0.99922	0.99968	0.99939
005	0.99974	0.99991	0.99847
015	0.99962	0.99975	0.99916

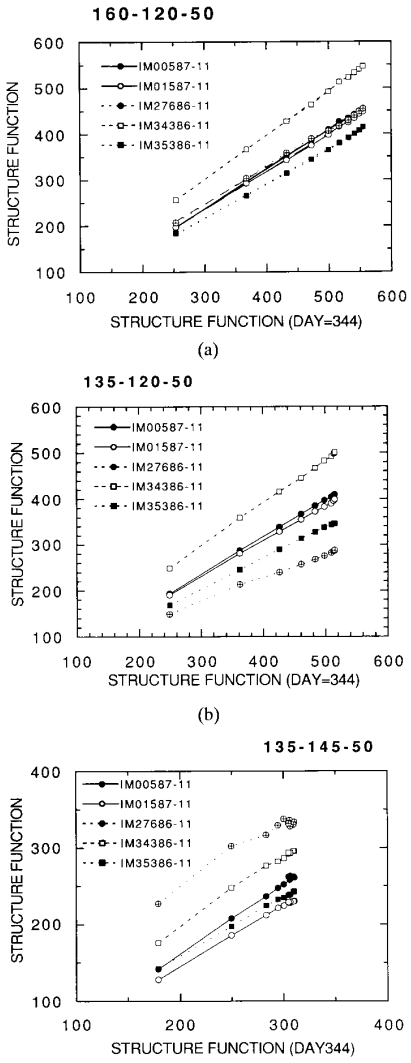

Fig. 9. The structure function for all days is plotted against the reference day, 344, for zones 1, 2, and 3 (a, b, and c). The slope of the lines are a function of the aerosol optical thickness.

lower for zone 3 (Table III). For day 276, starting at $d = 5$, the points deviate from a straight line, it is more obvious for zone 2 than for zone 1. This likely results from actual surface changes since day 276 corresponds to the end of the rainy season and

TABLE IV
COMPARISON BETWEEN THE PROPERTIES OF THE DDV, CONTRAST REDUCTION AND BRIGHTNESS METHOD [4]–[6] IN THE DERIVATION OF THE OPTICAL THICKNESS

Property/Method	DDV	Contrast Reduction	Brightness
Optical thickness derived	absolute	difference relative to a reference image	0.0-0.15
Range of surface reflectance for which the method applies	0.02±0.01 of DDV	any range as long as contrasts of at least $\Delta\rho = 0.1$ are present	
Main source of errors	assumed reflectance of the DDV scattering phase function	variation of surface reflectance from image to image, backscattering fraction of aerosol	variation of surface reflectance from image to image, scattering phase function
Special characteristics	algorithms used to detect DDV and aerosol uniformity (NDVI)	algorithms to detect variation in surface reflectance and structure, requires very good registration	requires good registration
Expected accuracy	$\Delta\tau$ = 0.1-0.2	$\Delta\tau$ = 0.1-0.2	$\Delta\tau > 0.2$
Application to atmospheric corrections	The eror due to uncertainty in the scattering phase function is canceled for correction of dark surfaces.	best applied to moderate to bright reflectances	limited application to pixels that changed greatly

is $\sim$ 3 months earlier than the other days. For zone 3, the linearity for any day is lower than for zones 1 and 2, possibly due to the lack of structure, a nonuniform atmosphere and/or to changes in the surface reflectance (Fig. 9(c)) as shown by the lower correlation coefficients. At this point, we do not know exactly the relative contributions causing the uncertainties.

The aerosol characteristics are taken from Shettle [33] background desert aerosol model which is similar to the D'Almeida model [34]. Since the geometrical conditions are known, the only remaining unknown is the aerosol optical thickness which is interpreted from the slopes of the $F^*s(d)$ plots (Fig. 9). Comparison between the three zones and the ground measurements shows scattered results for zone 3 and good agreement for zones 1 and 2 (Fig. 10). Based on these results we estimate the accuracy to be around 0.1 for the derivation of the aerosol optical thickness.

In addition to lack of structure, some of the discrepancies observed for zone 3 may result from inhomogeneities in the horizontal distribution of the aerosol optical thickness specifically within that zone. Furthermore, we have assumed the same aerosol model for all turbidity conditions. Shettle and D'Almeida found that the radiative properties of the aerosol change relative to the importance of the dust events. They suggest a higher value of the asymmetry parameter resulting from a larger particle size. Considering that, the extreme point of Fig. 10 would be closer to the 1:1 line but without more information on the atmosphere and ground conditions it is difficult to go further. An complete assessment by a systematic study of the zone is currently in progress [30].

IV. DISCUSSION AND IMPLICATIONS OF THE RETRIEVAL METHODS

The two aerosol optical thickness retrieval methods evaluated in this paper offer complimentary applications and have about the same retrieval accuracy for the conditions investigated here. Both are substantial improvements over the simple brightness method for the conditions in which they apply in that methodologies can be developed for retrieving aerosol optical thickness based on the radiative transfer equation (1)). Their geographic application is much greater, and their expected accuracy is better than the brightness method (Table IV). The DDV method is absolute and can be used on any image(s) with an area-of-interest spatial distribution of 1 pixel size DDV's. The contrast reduction method returns absolute values only when the analysis is anchored to a reference image of known aerosol optical thickness and thereby requires multidate imagery. The accuracy of retrieval for the DDV and Contrast Reduction methods appears to be about equal, 0.1–0.2, compared to > 0.2 for the brightness method. The DDV method may provide aerosol optical thickness over a portion of the world completely or partially covered by green forests. The contrast reduction method may be used to retrieve aerosols in semiarid and arid regions where forests do not exist, for transition areas of scattered forests where some DDV might occur and for seasonal or deciduous forests in which DDV is not present. In short, the methods have complimentary applications with possible overlap.

Our initial results indicate the DDV approach for retrieving the aerosol optical thickness is possible for the sites selected and, with further enhancements to the techniques and improved ground truth, will likely be applicable in areas with substantial anthropogenic surface and atmospheric disturbances. The results for the sites selected indicate the method using the 3.75-μm band is better than the NDVI method due to the insensitivity to the aerosol optical thickness, provided good cloud and cloud shadow screening is available. However, the NDVI approach should not be abandoned since other conditions exist in which the screened brightness temperature of the 3.75-μm band may be influenced by elevation and slope orientation or a different observation time (e.g., the NOAA morning satellites). Additionally the NDVI method may be used in concert with the traditional maximum value composite approach [19]. During the compositing period (typically, 1–4 weeks) the maximum NDVI is chosen on a pixel by pixel basis for daily data regardless of date. The selected data are typically near nadir viewing, are less cloud and water vapor contaminated, and have a smaller aerosol loading than individual days. Therefore, a trend toward uniformity of the aerosol loading and water vapor distribution in the composite image is likely. The NDVI method may be readily applicable and provide a computational advantage for this standard processing procedure as it would not introduce another band of data.

Further investigations are needed to improve the retrieval methods. The NDVI technique, for example, must used in a boxed grid for individual dates in which the assumption of

aerosol and water vapor uniformity and *a priori* DDV fraction is met. This may be manifested as variably sized grids within a scene which may change dimension from image to image and from one date to the next. We expect the methods could be improved by incorporating a water vapor correction for channel 3 and a Rayleigh and ozone correction for channel 1 prior to screening for DDV.

The following recommendations are suggested to improve our understanding of the aerosol retrieval from the AVHRR DDV method:

1) A lack of ground (atmospheric) truth limits our ability to set precise limits for the NDVI and 3.75- μm techniques. Future data sets must include knowledge of surface reflectance under varying conditions, aerosol model, water vapor, and aerosol optical thickness;
2) Because of the likelihood of subpixel clouds under cumulus formations, a technique to estimate their radiance contribution is necessary;
3) The 2% reflectance of DDV in the visible and 3.75-μm bands should be investigated from satellite and ground;
4) 2 and 3 will be useful for making a correction for the reflective component of the 3.75-μm band due to subpixel clouds.
5) A method of determining the minimum size box for the NDVI retrieval which contains DDV and has spatial uniformity of aerosols is necessary.
6) An ozone and Rayleigh correction for band 1, Rayleigh and water vapor correction for band 2, and water vapor correction for band 3 prior to the retrieval process should improve the results.

The contrast reduction method also shows very positive results when good structure was apparent within a zone and failed when structure was poor. Methodologies to determine adequate structure from the image rather than trial and error are required. Other work is continuing to determine invariant targets from the imagery. The correlation coefficient presented in Table III seems a good first approach. Additionally, problems of determining zone size and distance (d) are being addressed. Finally the applicability of the method is compromised by the spatial resolution of the satellite sensors. The requirement of aerosol uniformity and invariance of the target from one date to the next are compromised with coarser resolution satellite data. Therefore, an optimum zone size must balance the satellite sensor resolution with surface and atmospheric characteristics.

We have demonstrated the potential for applying the technique in an arid area having a predominantly bright surface. The method has potential in forested areas where ground cover reflectance is typically much lower. Full testing of the technique is difficult due to the paucity of adequate ground truth data sets. As these data become available, further investigation is required to evaluate this method under varying covertypes and compare it to the DDV method if possible.

Studies are continuing to improve the methods and determine which are appropriate for the existing conditions and in transition zones where neither DDV nor arid surface features dominate. Additionally, the methods are being evaluated for 4-km GAC pixel resolution data

ACKNOWLEDGMENT

The authors thank Dr. Ghassam Asrar for supporting this research through the NASA headquarters Remote Sensing Science Program.

REFERENCES

[1] D. Tanré, B. N. Holben, and Y. J. Kaufman, "Atmospheric correction algorithm for NOAA-AVHRR products: Theory and application," *IEEE Trans. Geosci. Remote Sensing*, vol. 30, pp. 000–000, March 1992.
[2] M. Griggs, "Measurements of atmospheric aerosol optical thickness over water using ERTS-1 data," *J. Air Pollut. Control Ass.*, vol. 25, pp. 622–626, 1975.
[3] C. R. N. Rao, E. P. McClain, and C. C. Stowe, "Remote sensing of aerosols over the oceans using AVHRR data theory, practice and applications," *Int. J. Remote Sensing*, vol. 10, nos. 4–5, pp. 743–749, 1989.
[4] Y. J. Kaufman and C. Sendra, "Algorithm for automatic atmospheric corrections to visible and near-IR satellite imagery," *Int. J. Rem. Sens.*, vol. 9, pp. 1357–1381, 1988.
[5] D. Tanré, P. Y. Deschamps, C. Devaux, and M. Herman, "Estimation of Saharan aerosol optical thickness from blurring effects in Thematic Mapper data," *J. Geophys. Res.*, pp. 15955–15964, 1988.
[6] R. S. Fraser, Y. J. Kaufman, and R. L. Mahoney, "Satellite measurements of aerosol mass and transport," *Atmos. Environ.*, vol. 18, pp. 2577–2584, 1984.
[7] Y. J. Kaufman, R. S. Fraser, and R. A. Ferrare, "Satellite measurements of large-scale air pollution methods," *J. Geophys. Res.*, vol. 95(D7), pp." 9895–9909, 1990.
[8] R. Ferrare, R. S. Fraser, and Y. J. Kaufman, "Satellite measurements of large-scale air pollution measurements of forest fire smoke," *J. Geophys. Res.*, vol. 95(D7), pp. 991 1–9925, 1990.
[9] F. G. Hall, D. E. Strebble, J. E. Nickeson, and S. F. Goetz, "Radiometric rectification: Toward a common radiometric response among multi-date, multi-sensor images," *Remote Sens. Environ.*, vol. 35, pp. 1–27, 1991.
[10] Y. Mekler H. Quenzel, G. Ohring, and I. Marcus, "Relative atmospheric aerosol content from ERTS observations," *J. Geophys. Res.*, vol. 82, pp. 967–972,1 977.
[11] P. Koepke, and H. Quenzel, "Turbidity of the atmosphere determined from satellite calculation of optimum viewing geometry," *J. Geophys. Res.*, vol. 84, pp. 7847–7855, 1979.
[12] K. T. Kriebel, "Reflection properties of vegetated surfaces: Tables of measured spectral biconical reflectance factors," Munchener Universitats-Schriften, Meteorologisches Ins., Wissenschaftl. Mitteilung, vol. 29, 1977.
[13] D. W. Deering and T. F. Eck, "Directional radiance distributions above and within a forest canopy," in *Proceedings of IGARSS '90, 10th Annual International Geoscience and Remote Sensing Symposium*, vol. 1, pp. 879–882, 1990.
[14] D. S. Kimes, W. W. Newcomb, R. F. Nelson, and J. B. Schutt, "Directional reflectance distributions of a hardwood and pine forest canopy," *IEEE Trans. Geosci. Remote Sensing*, vol. GE-24, pp. 281–297, 1986.
[15] J. Kleman, "Directional Reflectance Factor distributions for two forest canopies," *Remote Sens. Environ.*, vol. 23, pp. 83–96, 1987.
[16] Y. J Kaufman,, A. Setzer, D. Ward, D. Tanré, B. N. Holben, P. Menzel, M. C. Pereira, and R. Rasmussen, "Biomass Burning Airborne and Spaceborne Experiment in the Amazonas (BASE-A)," *J. Geophys. Res.*, in press, 1992.
[17] Y. J. Kaufman, "Measurements of the aerosol optical thickness and the path radiance — implications on aerosol remote sensing and atmospheric corrections," *J. Appl. Meteorol.*, in press, 1992
[18] C. J. Tucker, "Red and photographic infrared linear combinations for monitoring vegetation," *Remote Sens. Environ.*, vol. 8, pp. 127–150, 1979.
[19] B. N. Holben, "Characteristics of maximum-value composite images from temporal AVHRR data," *Int. J. Remote Sens.*, vol. 7, pp. 417–434, 1986.
[20] B. N. Holben and R. S. Fraser, "Red and near intrared response to off nadir viewing," *Int. J. Remote Sens.*, vol. 5, pp. 145–160, 1984.
[21] T. Lee and Y. J. Kaufman, "The effect of surface nonlambertianity on remote sensing," *IEEE Trans. Geosci. Remote Sensing*, vol. GE-24, pp. 699–708, 1985.
[22] A. Arking and J. D. Childs, "Retrieval of cloud cover parameters from multispectral satellite images," *J. Clim. Appl. Meteorol.*, vol. 24, pp. 322–333, 1985.

[23] A. G. Kerber and J. B. Schutt, "Utility of AVHRR Channels 3 and 4 in land cover mapping," *Photogrammetr. Eng. Rem. Sens.*, vol. 52, pp. 1877–1883, 1986.
[24] J. Malingreau and C. J. Tucker, "Large scale deforestation in the Southeastern Amazon Basin of Brazil'," *Ambio*, vol. 17, pp. 49–55, 1988.
[25] C. J. Tucker, B. N. Holben, and T. E. Goff, "Intensive forest clearing in Rondonia, Brazil, as detected by satellite remote sensing," *Remote Sens. Environ.*, vol. 15, p. 255, 1984.
[26] K. T. Whitby, "The physical characteristics of sulfur aerosols," *Atmos. Environ.*, vol. 12, pp. 135–159, 1978.
[27] E. P. Shettle, and R. W. Fenn, "Models for the aerosol of the lower atmosphere and the effect of humidity variations on their optical properties," AFGL-TR790214, Opt. Phys. Div., Air Force Geoph. Cab., Hanscom AFB MA, 1979.
[28] B. N. Holben, Y. J. Kaufman, A. Setzer, D. Tanré, and D. E. Ward, "Optical properties of aerosols from biomass burning in the tropics, BASE-A," presented at the Chapman Conference on Biomass Burning, Williamsburg, VA, Mar. 1990.
[29] B. N. Holben, T. Eck, and R. S. Fraser, "Temporal and spatial variability of aerosol optical depth in the Sahel region in relation to vegetation remote sensing," *Int. J. Remote Sens.*, vol. 12, no. 6, pp. 1147–1163, 1991.
[30] D. Tanré and E. Vermote, "Retrieval of aerosol optical thickness over land," manuscript in preparation, 1992.
[31] Y. J. Kaufman, C. J. Tucker, and I. Y. Fung, "Remote sensing of biomass burning in the tropics," *Advances in Space Research*, vol. 9, no. 7, pp. (7)265-(7)268, 1989.
[32] D. Tanré, C. Deroo, P. Duhaut, M. Herman, J. J. Morcrette, J. Perbos, and P. Y. Deschamps, "Description of a computer code to simulate the satellite signal in the solar spectrum: 5S code," *Int. J. Remote Sensing*, vol. 11, pp. 659–668, 1990.
[33] E. P. Shette, "Optical and radiative properties of a desert aerosol model," in *Proc. Symposium on Radiation in the Atmosphere,* G. Fiocco, Ed. Hampton, VA: Deepak Publishing, 1984, pp. 74–77.
[34] G. A. D'Almeida, "On the variability of desert aerosol radiative characteristics," *J. Geophys. Res.*, vol. 92, pp. 3017–3026, 1987.

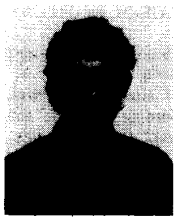

Didier D. Tanré received the M.Sc. degree in physics in 1975 and the thesis in atmospherics physics, "Thèse de 3ème Cycle" and "Doctorat d'Etat", in 1977 and 1982, respectively, from University of Lille, France.

Since 1982, he has been employed at the laboratoire d'Optique Atmosphérique, Lille, France, as a CNRS (Centre National de Ia Recherche Scientifique) researcher and is currently on leave at NASA Goddard Space Flight Center as a NRC Research Associate. His activities cover radiative transfer modeling though realistic atmospheres both theory and applications. His interests also include remote sensing of the atmospheric properties from satellite and ground based observations as well as atmospheric effects in satellite imagery of the Earth's surface.

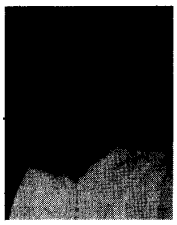

Virginia Kalb received the M.S. degree in mathematics at the University of Maryland in 1977.

Since then she has taken many graduate courses in computer science and is currently working with *X* windows applications.

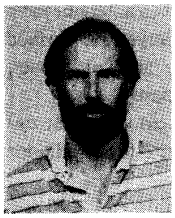

Brent Holben received the B.S. degree in agronomy at the University of Idaho in 1972 and the M.S. degree in bioclimatology at Colorado State University in 1975.

He worked for 2 years at the Puerto Rico Nuclear Center in biometeorology before joining Goddard Space Flight Center's Biospheric Sciences Branch in 1978. Since then Holben has worked on short wave remote sensing of green vegetation using ground and satellite systems and, more recently, remote sensing of aerosol properties for application to atmospheric correction.

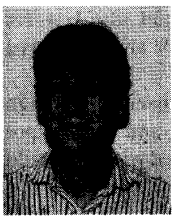

Eric Vermote received the Engineer degree in computer science in 1987 from Ecole des Hautes Etudes Industrielles (H.E.I.), Lille, France, and the Ph.D. degree in atmospheric optics from the University of Lille, France in 1990.

He is currently a visiting scientist at the University of Maryland and works with the MODIS Team on the atmospheric correction problem at NASA/Goddard Space Flight Center, MD.

Yoram J. Kaufman received the B.Sc. and M.Sc. degrees in physics from the Technion -Israeli Inst. of Technology, Israel, in 1972 and 1974, respectively, and the Ph.D. degree from the Tel-Aviv University in 1979.

He joined NASA Goddard Space Flight Center in 1979 on an NRC fellowship award. He is presently employed by the NASA Goddard Space Flight Center, Greenbelt, MD. His present work includes theoretical and experimental research in atmospheric science, radiative transfer, and remote sensing. His research activity include remote sensing of aerosol and clouds; atmospheric correction of satellite imagery of the earth's surface; interaction of aerosols and clouds, and their climatic impact; remote sensing of emissions from biomass burning in the tropics; and calibration of satellite sensors. He conducts field experiments, that include measurements from aircraft and from the ground of the aerosol properties (smoke aerosol, dust, and anthropogenic aerosol) and their effect on radiative transfer. He is a member of the Earth Observing System—MODIS team. Three of his papers on properties of CO_2 lasers and saturable absorbers, written from his work in the Technion, were selected for SPIE milestone Series "of outstanding papers from the world literature on optical and optoelectronic science: Selected Papers. on CO_2 Lasers."